International Journal of the Physical Sciences Vol. 6(1), pp. 52-64, 4 January, 2011
Available online at http://www.academicjournals.org/IJPS
DOI: 10.5897/IJPS10.643
ISSN 1992 - 1950 ©2011 Academic Journals

Full Length Research Paper

Zero padded suffix aided subspace-based narrowband interference detected adaptive channel estimation for MB-OFDM UWB systems

S. M. Riazul Islam[1] and Kyung Sup Kwak[2]*

[1]Inha University, 253, Yong-hyun dong, Nam-gu, Incheon, 402-751, South Korea.
[2]6-142, UWB-ITRC, Inha University, 253, Yong-hyun dong, Nam-gu, Incheon, 402-751, South Korea.

Accepted 04 January, 2011

The ECMA-368 standard specifies multiband orthogonal frequency division multiplexing (MB-OFDM) as the definitive technology for high rate ultra-wideband (UWB) communications. Like other wireless systems, the performance of a correct data signals detection and decoding in MB-OFDM UWB is reduced by narrowband interference (NBI). A more specific problem of severity arises when interferences are present during the channel estimation process, since this eventually results to severe degradation in the performance of signal reconstruction in the whole packet layer convergence protocol (PLCP) and service data unit (PSDU). In this article, we propose an improved channel estimation technique for OFDM-based UWB systems in presence of NBI. Several steps have been carried out to achieve this purpose. First, the location of center frequency of NBI is found out through zero padded suffix (ZPS) aided subspace-based method. Secondly, we propose an adaptive band select and replace (ABSR) scheme to eliminate NBI based on frequency-domain redundancy (FR) property we introduce into preamble symbols during transmission. Thirdly, we perform least-square (LS) channel estimation on NBI-free received preamble symbols to get the estimated channel at each subcarrier. Fourthly, low rank least square minimum mean squared error (LMMSE) channel estimation is performed using this LS channel estimation. Lastly, Blackman windowing is applied on low rank LMMSE channel to reduce the spectral leakage and thus to increase the channel estimation accuracy. Link level simulation (LLS) urges that our proposed technique has improved performances.

Key words: Ultra-wideband (UWB), channel estimation, multiband orthogonal frequency division multiplexing (MB-OFDM), narrowband interference (NBI), ECMA-368, wireless personal area network (WPAN).

INTRODUCTION

Ultra-wideband (UWB) technology has already been well documented as a most suitable candidate for short-range multiple access communications. Reasons they are preferred include potential for high data rate, low susceptibility to multi-path interference, potential small size and processing power, together with low equipment cost as well as high precision ranging and localization. UWB technology can enable a wide variety of applications in wireless communications, networking, radar imaging and localization systems. UWB technology employing orthogonal frequency division multiplexing (OFDM) is termed MB-OFDM UWB. The popularity of MB-OFDM UWB system continues to grow as the physical layer (PHY) of wireless personal area network (WPAN), especially for high data rate applications in home networks. MB-OFDM has already been fixed in the standard ECMA-368 (ECMA International, 2008) for high rate UWB.

The MB-OFDM systems have the following unique characteristics (Li et al., 2008) if compared to conventional OFDM systems: a) different channel responses and channel energies across different bands, b) different carrier frequency offsets (CFOs) across

*Corresponding author. E-mail: kskwak@inha.ac.kr. Tel: +82-032-860-7416.

different bands, c) the use of zero padding (ZP) instead of cyclic prefix (CP), d) interplay between the timing and the frequency hopping. These characteristics provide diversity components and additional design constraints, and hence, should be taken into account in the designs of synchronization, channel estimation and equalization. Over the past few years, a lot of research has been conducted to determine rewarding technological means towards the success of MB-OFDM UWB technology, of which channel estimation was prominent. Considerable research efforts have been dedicated to propose/investigate new channel estimation techniques that could satisfy the crucial MB-OFDM system requirements. However, a few of them are preamble-based approaches; preamble-based approaches are the essential means, in the guidelines of ECMA-368, for synchronization, and channel estimation.

The comprehensive study (Islam and Kwak, 2010) presents an overview of channel estimation techniques proposed/investigated for MB-OFDM systems with emphasis on their strengths and weaknesses. The work in (Li et al., 2008) develops carrier frequency offset (CFO)-assisted CIR estimator with imperfect timing offset. Authors in (Fan et al., 2005) apply rectangular windowing, with an adaptive length, on discrete Fourier transform (DFT) estimator to get improved estimation performance. The work in (Png et al., 2008) introduces adaptive filter in the frequency-domain to reduce the mean square error (MSE) of the estimated channel. Authors in (Shin et al., 2007) propose low rank linear minimum mean square error (LMMSE) channel estimation with variable rank. However, these works (Li et al., 2008; Fan et al., 2005; Png et al., 2008; Shin et al., 2007) assume interference-free environments; preambles are not hindered by interference.

The work in (Li et al., 2006) develops practical approaches for channel estimation and interference suppression. Yet the interference suppression method is based on interference averaging. Authors in (Tasi et al., 2008) propose an adaptive channel estimation method in presence of multi-access interference (MAI); they apply time-domain redundancy (TR) property. Yet they do not study the feasibility of estimation accuracy in presence of NBI. A joint NBI detection and channel estimation is found in (Hadaschik et al., 2007); this is an iterative approach that finds the subcarrier with maximum power to consider the center frequency of the NBI. Conversely, the approach needs relatively higher computational complexity. Moreover, this method cannot detect all NBI-affected subcarriers.

In our previous work (Islam and kwak, 2010), we propose energy-efficient channel estimation in presence of both MAI and NBI. However, this involves a threshold-based NBI detection approach; the estimation performance could significantly be altered, due to bad choice of threshold. Articles (Kelleci et al., 2008; Popescu et al., 2007; Shi et al., 2007; Snow et al., 2009) and references therein present in-depth analysis to assess the impact of NBI on the performance of a MB-OFDM UWB receiver. They also put forward useful NBI mitigation techniques. However, these works like focusing on system as a whole rather than channel estimation, a part of system. To the best of our knowledge, we do not find any other useful work that provides satisfactory estimation performances in presence of NBI. In this paper, we propose an improved channel estimation technique for MB-OFDM UWB systems in presence of NBI.

ECMA-368, CHANNEL ESTIMATION AND NBI

According to the ECMA-368 standard, the MB-OFDM approach divides the UWB spectrum into 14 bands, each with a bandwidth of 528 MHz. The first 12 bands are then grouped into 4 band groups consisting of 3 bands, and last two bands are grouped into a fifth band group. Figure 1 is an instant example of the transmitted radio frequency (RF) band plan for a MB-OFDM system. This example implicitly assumes the time-frequency coding (TFC) is performed across just three OFDM symbols. Accordingly, the first OFDM symbol is transmitted on band 1, the second OFDM symbol is transmitted on band 2, the third OFDM symbol is transmitted on band 3, the forth OFDM symbol is transmitted on band 1, and so on. A total of 110 sub-carriers (100 data carriers and 10 guard carriers) are used per band. In addition, 12 pilot sub-carriers allow for coherent detection. The 10 guard carriers used for mitigating inter symbol interference (ISI) are located on either edge of the OFDM symbol. A 70.08ns zero-padded suffix (ZPS) is inserted at the end of each ODM symbol to aid multipath interference mitigation and settling times of the transmitter (T_X) and receiver (R_X).

To operate the PHY service interface to the media access control (MAC) service, a packet layer convergence protocol (PLCP) sublayer is defined. PLCP sublayer provides a method for converting a PLCP service data unit (PSDU) into a PLCP packet data unit (PPDU), resulting in the PPDU being composed of three components as shown in Figure 2(a); the PLCP preamble, PLCP header, and the PSDU. The PLCP preamble is the first component of the PPDU and can be further decomposed into packet/frame synchronization (PFS), and channel estimation (CE) sequences. The goal of the PLCP preamble is to aid the receiver in timing synchronization, carrier-offset recovery, and channel estimation. The PFS is either 12 (burst mode) or 24 (standard mode) zero autocorrelation stored time-domain bursts with the same timing as OFDM frames. The channel estimation sequence is actually defined in the frequency-domain and an inverse fast Fourier transform (IFFT) process can be used to convert to the required time-domain for transmission. Two OFDM symbols are used as a channel estimation sequence for each band. Thus, six OFDM symbols are needed for channel estimation as the MB-OFDM system employs hopping over a maximum of 3 bands.

The radio channel in mobile radio systems is usually multi-path fading channel that causes ISI in the received signal. Many kinds of equalizers can be used to remove the ISI from the signal. However, these detectors require knowledge on the channel impulse response (CIR) that can be provided by a separate channel estimator. A mathematical and/or statistical method building the channel estimator is termed the channel estimation technique. This technique allows the receiver to approximate the impulse response of the channel and explain the behavior of the channel. So, channel estimation is essential in order to have successful information decoding in the receiving side of the communication system. There

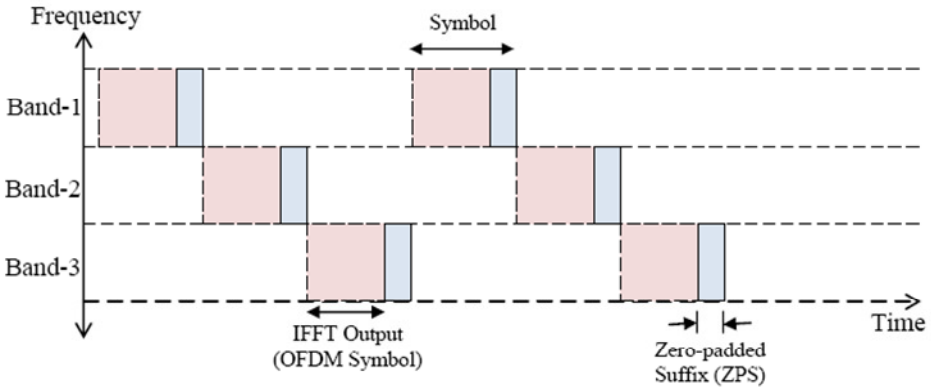

Figure 1. Realization of a transmitted RF signal for a MB-OFDM system using three bands.

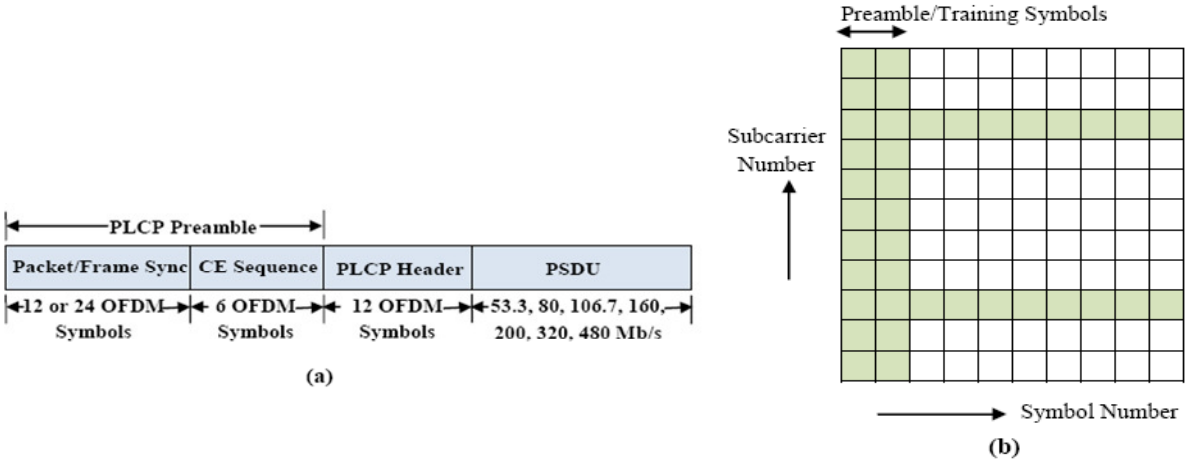

Figure 2. (a) Structure of PLCP packet data unit (PPDU) (b) Example of a packet with preambles.

are many methods of channel estimation techniques. The selection of a particular method to be used depends upon the communication environment, channel, and transmission systems. For the specific problem of channel estimation in packet transmission systems, with slow-fading channel, the most appropriate approach seems to be the use of a preamble (training symbols) consisting of one or more known OFDM symbols (Nee et al., 2000).

This approach is sketched in Figure 2(b). The figure shows the time-frequency grid with subcarriers on the vertical axis and symbols on the horizontal axis. All shaded subcarriers are pilots. The packet starts with two OFDM symbols for which all data values are known. These training symbols can be used to obtain channel estimates. After the first two training symbols, Figure 2(b) shows two pilot sub-carriers within the data symbols. These pilots are not meant for channel estimation, but for tracking the remaining frequency offset after the initial training. The choice of the number of training symbols is a tradeoff between a short training time and a good estimation performance. ECMA-368 uses two training symbols, as discussed in the early part of this section, for each sub-band.

In the study of UWB system, narrowband implies bandwidth under consideration is “sufficiently” narrow compared to the UWB bandwidth. A wideband system, by its nature, interferes with the existing narrowband services in the same frequency band and in turn, the narrowband signals act as interferers to wideband system. This interference is termed narrowband interference (NBI). NBI reduces the performance of a correct data signal detection and decoding. A more specific problem of severity arises when this is present during the channel estimation process, since this eventually results severe degradation in the performance of signal reconstruction in the entire data packet/frame.

The transmitted power level of UWB systems is limited to -41.3 dBm/MHz and can be spread over a huge bandwidth 7.5 GHz, according to federal communications commission (FCC). Such a noise floor operation facilitates the coexistence of UWB devices with other services as IEEE 802.11 wireless local area network (WLAN), IEEE 802.16 worldwide interoperability for microwave access (WiMAX), etc. Due to their low transmission power and huge reception bandwidth, UWB systems are subject to intentional and unintentional NBIs (Shi et al., 2007).

SYSTEM MODEL

The MB-OFDM system under consideration is illustrated in Figure 3. In this model, we do not consider scrambling, puncturing and

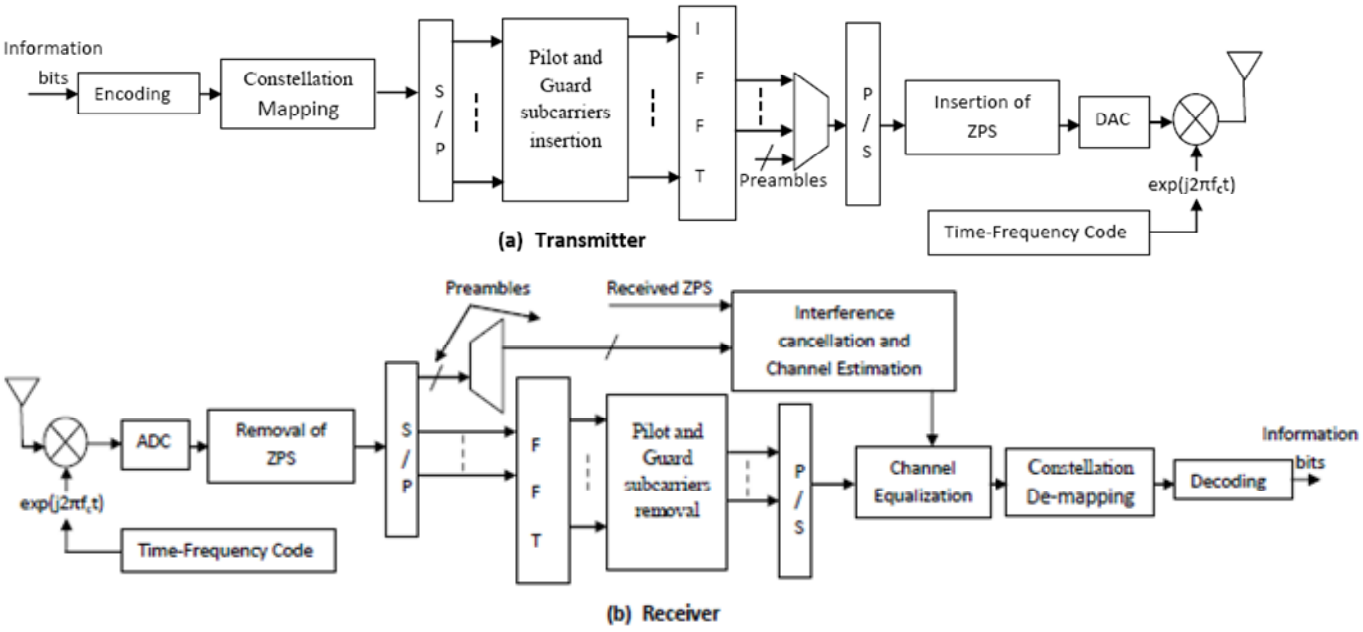

Figure 3. MB-OFDM system model.

interleaving for simplicity. Accordingly, the system does not guarantee the information security, compact redundancy and burst-error handling. However, these are not important for our study, since they do not affect channel estimation performances. The information bits, with average power equal to E_c, are fed into a convolution encoder with rate, R, to provide redundancy against bad channel effects. The output of encoder is then mapped onto each subcarrier based on quadrature phase shift keying (QPSK) constellation with average power equal to E_s. The output of the constellation mapper is then passed through serial-to-parallel (S/P) converter and pilot and guard subcarriers insertion block. The frequency-domain data symbols located on the subcarriers are denoted by $\bar{D}$ and given by:

$$\bar{D} = [D[k]]^T = [D_0, D_1, \dots, D_{N-1}]^T, \quad (1)$$

Where $(.)^T$ denotes the transpose operator and *N* be the number of subcarriers constituting the OFDM symbol. Note that the average power of the coded data on each tone is given by $E_c = RE_s$. The data symbols are subsequently modulated into time-domain samples using IFFT:

$$\bar{d} = [d[n]]^T = [\frac{1}{N}\sum_{k=0}^{N-1} D[k].e^{-2\pi nk/N}]^T, \quad n = 0,1,\dots,N-1, \quad (2)$$

A ZPS of Z samples is appended at the end of $\bar{d}$ to give:

$$\bar{d}_{ZPS} = \left[d_0, d_1, \dots, d_{N-1}, d_N, d_{N+1}, \dots, d_{N+Z-1}\right]^T, \quad (3)$$

The ZPS is used to mitigate the effects of ISI and inter carrier interference (ICI) caused by the channel. The digital time-domain signal given in Equation (3) is then converted to analog signal, using digital-to-analog converter (DAC), for transmission. The output of DAC is multiplied by one of the RF frequency bands scheduled by TFC, as discussed in the previous section of this paper. However, we will present the analysis for the baseband digital part only, since we avoid RF signal processing for simplicity. The channel that we are interested in is IEEE 802.15.3a UWB RF channel model described in (Molisch et al., 2003) is given by:

$$h(t) = X\sum_{l=0}^{L_h}\sum_{k=0}^{K}\alpha_{k,l}\delta(t - T_l - \tau_{k,l}), \quad (4)$$

Where T_l, $\tau_{k,l}$ and X are random variables representing the delay of the l-th cluster, the delay (relative to the l-th cluster arrival time) of the k-th multipath component of the l-th cluster and the log-normal shadowing, respectively.

The channel coefficients are defined as a product of small-scale and large-scale fading coefficients, that is, $\alpha_{k,l} = p_{k,l}\,\xi_l\beta_{k,l}$ where $p_{k,l}$ takes on equiprobable ± 1 to account for signal inversion due to reflections, and $\left\{\xi_l\beta_{k,l}\right\}$ are log-normal distributed path gains. Then we have $E\left[\alpha_{k,l}(T_l,\tau_{k,l})\right] = 0$ and $E\left[\left|\alpha_{k,l}(T_l,\tau_{k,l})\right|^2\right] = \Omega_0 e^{-T_l/\Gamma} e^{-\tau_{k,l}/\gamma}$. Γ and γ are the cluster decay factor and ray decay factor, respectively. With different parameters, four typical environments are defined; they are CM1, CM2, CM3 and CM4. Note that CMj stands for Channel Model j. Details of the channel model are referred to (Molisch et al., 2003). Assuming perfect timing and frequency synchronization, the received time-domain signal (with ZPS) is given by:

$$\bar{y}_{ZPS} = \bar{d}_{ZPS} * \bar{h} + \bar{\imath}_{ZPS} + \bar{w}_{ZPS}, \quad (5)$$

Where (*) denotes the convolution operator and $\bar{h}$ is the channel response vector. $\bar{w}_{ZPS}$ is the $N+Z \times 1$ vector of Gaussian noise samples with zero-mean and variance equal to σ_w^2, and $\bar{\imath}_{ZPS}$ is the $N+Z \times 1$ vector of interference samples.

The ZPS is removed from the received signal through overlapped-and-add (OLA) process, giving:

$$\bar{y} = \bar{d} * \bar{h} + \bar{\imath} + \bar{w}, \quad (6)$$

Where $\bar{\imath}$ is the $N \times 1$ vector of interference samples and $\bar{w}$ is the $N \times 1$ vector of additive white Gaussian noise (AWGN) samples with the same distribution as $\bar{w}_{ZPS}$. This signal is then converted into the frequency-domain with the fast Fourier transform (FFT), to give:

$$\bar{Y} = D\bar{H} + \bar{I} + \bar{W}, \quad (7)$$

Where D is the $N \times N$ diagonal matrix with the elements of $\bar{D}$ as diagonal elements that is., $D = diag(D_0, D_1, \ldots, D_{N-1})$. The symbols $\bar{H}$, $\bar{I}$ and $\bar{W}$ are the frequency-domain representations of $\bar{h}$, $\bar{\imath}$, and $\bar{w}$ respectively. We assume the bandwidth of the NBI is sufficiently narrow compared with that of the sub-band of UWB system. This assumption allows us to model NBI as a single tone sinusoid (Zhang et al., 2004) and given by:

$$i[n] = \alpha e^{j(\omega n + \emptyset)} \quad (8)$$

Where α, ω, and $\emptyset$ are the amplitude, frequency, and phase offset of the NBI. If the NBI frequency coincides with a subcarrier frequency, it will interfere only with that subcarrier. However, this is usually not true. When the interference is non-orthogonal, the interference power is spread across all the tones and spectral leakage occurs. As the interference power is increased, a larger set of tones are severely degraded by the interference. Subcarriers in the vicinity of NBI are more strongly affected. While data symbol is passed through the channel equalization block, it requires CIR from channel estimation block. For our system model, CIR is estimated using preamble symbols.

Preambles must be free from NBI, since NBI affected preambles (in a similar manner in which data symbols are affected) will provide bad estimate of CIR. This will in turn result severe performance degradation in channel equalization and in data decoding. After synchronization sequence, preamble symbol of channel estimation sequence is sent to the receiver. So, the corresponding equations will be modified, during channel estimation, by plugging the preamble symbol instead of data symbol. Suppose, frequency-domain preamble symbol is denoted by X and given by:

$$\bar{X} = [X[k]]^T = [X_0, X_1, \ldots, X_{N-1}]^T, \quad (9)$$

and the time-domain representation of X is denoted by $\bar{x}$. Then Equation (6), for the received time-domain preamble symbol, can be written as:

$$\bar{y} = \bar{x} * \bar{h} + \bar{\imath} + \bar{w} = \bar{r} + \bar{\imath} + \bar{w}, \quad (10)$$

Where $\bar{x} * \bar{h}$ is denoted as $\bar{r}$. Similarly, Equation (7) will be modified, to give frequency-domain received preamble symbol, as:

$$\bar{Y} = X\bar{H} + \bar{I} + \bar{W} = \bar{R} + \bar{I} + \bar{W} \quad (11)$$

Where $X\bar{H}$ is denoted as $\bar{R}$. Note that the frequency-domain preamble sequence that is $\{X_0, X_1, \ldots, X_{N-1}\}$ is defined in ECMA-368 standard. We need an IFFT operation, where necessary, to convert $\bar{X}$ to $\bar{x}$, since ECMA-368 standardizes preamble sequences in frequency-domain. Conversely, FFT operation is applied on $\bar{x}$ to revert back to $\bar{X}$.

PROPOSED NBI-FREE CHANNEL ESTIMATION

We introduce frequency-domain redundancy (FR) into two channel estimation preamble symbols before transmission. This is done by decimating the time-domain preamble symbols by a factor of 2. The row vector representation of time-domain preamble sequence, denoted by $x[n]$, can be obtained by the IFFT operation on (9) as:

$$x[n] = \frac{1}{N}\sum_{k=0}^{N-1} X[k] \times e^{j2\pi nk/N}, \quad n = 0,1, \ldots, N-1 \quad (12)$$

Applying FFT operation on Equation (12), we get frequency-domain preamble sequence:

$$X[k] = \sum_{n=0}^{N-1} x[n] \times e^{-j2\pi nk/N}, \quad k = 0,1, \ldots, N-1 \quad (13)$$

By decimating the samples in $x[n]$ by a factor of 2, we get the corresponding frequency-domain preamble symbol as:

$$X_{even}[k] = \sum_{n=0}^{M-1} x[2n] \times e^{-\frac{j2\pi(2n)k}{2N}}, \quad k = 0,1, \ldots, N-1, \quad (14)$$

Where $M = N/2$. The subscript "$even$" is used, since even-numbered samples have been used during decimation. The odd-numbered samples are set to zero. It must be noted that the last half of $X_{even}[k]$ is the duplication of first half, since:

$$X_{even}[k+M] = \sum_{n=0}^{M-1} x[2n] \times e^{\frac{-j2\pi(2n)(k+M)}{2N}} - \sum_{n}^{M-1} x[2n] \times e^{\frac{-j2\pi(2n)k}{2N}} \times e^{j2\pi n} - X_{even}[k], \; k = 0,1, \ldots, M-1, \quad (15)$$

Therefore, we have the FR property in the channel estimation preamble symbols. Similarly, the odd-numbered of samples can also be used to get FR property. In this article, we use even-numbered samples. For the sake of symbolic simplicity, we avoid the subscript "$even$" in the rest of this article. Now, based-on this FR property, we will propose NBI elimination algorithm. However,

the algorithm requires some knowledge of NBI, especially the frequency. Let us present the technique to detect the NBI using ZPS-aided subspace-based method. This method using cyclic prefix is first proposed in (Frein et al., 2006). Employing a ZPS of length N_{ZPS}, the transmitted preamble signal is structured such that:

$$x[n] = x[n+N], \quad n = 0, \dots, N_{ZPS} - 1 \tag{16}$$

Assuming the length of ZPS is longer than the channel memory, we have:

$$y[n] = y[n+N], \quad n = L-1, L, \dots, N_{ZPS} - 1 \tag{17}$$

Where L is the length of channel memory and $y[n]$ is the nth received preamble sample. Suppose the number of samples used in the NBI estimation process is denoted by N_2 and $N_2 = N_{ZPS} - L + 1$. For each $n = L-1, L, \dots, N_{ZPS} - 1$, we define the sequence $q[n]$ as follows:

$$\begin{aligned} q[n] &\triangleq y[n+N] - y[n] \\ &= \alpha e^{j\theta}\left(e^{j\omega N} - 1\right)e^{j\omega n} + w[n], \end{aligned} \tag{18}$$

Where $w[n]$ is the nth sample of AWGN w. W define $L_2 = N_2 - P + 1$ vectors $\bar{q}$, each of size $(P \times 1)$, as follows:

$$\begin{aligned} \bar{q}[n] &= [\, q[n] \; q[n+1] \dots \; q[n+P-1] \,]^T \\ &= \alpha e^{j\theta_n}\left(e^{j\omega N} - 1\right)\sqrt{P}\,\bar{s} + \bar{w}[n], \end{aligned} \tag{19}$$

Where the span of $\bar{s} = \frac{1}{\sqrt{P}}[\; 1 \;\; e^{j\omega} \;\; e^{2j\omega} \;\; \dots \;\; e^{(P-1)j\omega} \;]^T$ is the signal space S and its orthogonal complement $S^{\perp}$ is the noise subspace. The $(P \times P)$ autocorrelation matrix of the vector $\bar{q}$ is by definition:

$$C_{\bar{q}} \triangleq E\{\bar{q}[n](\bar{q}[n])^H\}, \tag{20}$$

And can be written as the sum of a rank one matrix and the identity matrix I scaled by σ_w^2 as follows:

$$C_{\bar{q}} = \alpha^2 P\left|e^{j\omega N} - 1\right|^2 \bar{s}\bar{s}^H + \sigma_w^2 I, \tag{21}$$

Using eigenvalue decomposition (EVD), Equation (21) can be written as:

$$C_{\bar{q}} = (\bar{u}_{\bar{s}}\; \bar{U}_{\bar{w}}) \begin{pmatrix} \lambda + \sigma_w^2 & 0 & \dots & 0 \\ 0 & \sigma_w^2 & 0 & \vdots \\ \vdots & 0 & \ddots & 0 \\ 0 & \dots & 0 & \sigma_w^2 \end{pmatrix} \begin{pmatrix} \bar{u}_{\bar{s}}^H \\ \bar{U}_{\bar{w}}^H \end{pmatrix}, \tag{22}$$

Where $\lambda = \alpha^2 P\left|e^{j\omega N} - 1\right|^2$ and $\bar{u}_{\bar{s}} = \bar{s}$. We generate an estimate of $C_{\bar{q}}$ by time averaging:

$$\hat{C}_{\bar{q}} = \frac{1}{L_2}\sum_{n=L-1}^{N_{ZPS}-1} \bar{q}[n](\bar{q}[n])^H, \tag{23}$$

Performing the EVD of $C_{\bar{q}}$, the largest eigenvalue is denoted by ρ_0 and the others are donated by $\{\rho_1, \; \rho_2, \; \dots, \; \rho_{P-1}\}$. The noise variance σ_w^2 is estimated as:

$$\hat{\sigma}_w^2 = \frac{1}{P-1}\sum_{i=1}^{P-1} \rho_i \tag{24}$$

The eigenvector corresponds to the largest eigenvalue is denoted by:

$$\hat{\bar{s}} = [\hat{s}_0 \;\; \hat{s}_1 \;\; \dots \;\; \hat{s}_{P-1}]^T, \tag{25}$$

Since $s_n = \frac{1}{\sqrt{P}} e^{j\omega n}$, where $n = 0, 1, \dots, P-1$, we have $\frac{s_{n+1}}{s_n} = e^{j\omega}$, where $n = 0, 1, \dots, P-2$, and thus the frequency can be estimated as follows:

$$\hat{\omega} = \frac{1}{P-1}\sum_{n=0}^{P-2} Im\left\{ln\left(\frac{\hat{s}_{n+1}}{\hat{s}_n}\right)\right\}, \tag{26}$$

The largest eigenvalue $\lambda + \sigma_w^2$ allows estimating the amplitude of NBI as:

$$\hat{\alpha} = \sqrt{\frac{\rho_0 - \hat{\sigma}_w^2}{P\left|e^{j\omega N} - 1\right|^2}}, \tag{27}$$

Finally, the phase is estimated as:

$$\hat{\theta} = \frac{1}{N_2}\sum_{n=0}^{N_2-1} Im\left\{ln\left(\frac{\bar{q}[n].e^{j\Omega n}}{\hat{\alpha}(e^{j\omega N} - 1)}\right)\right\}, \tag{28}$$

Now, we are equipped to eliminate NBI from preambles. Not only the subcarrier nearest to the NBI frequency is hampered but also adjacent subcarriers are affected. How many subcarriers will be considered as NBI-contaminated depends on signal-to-interference ratio (SIR) and is a system design issue. We convert the received time-domain preamble symbol (IFFT symbol) by FFT. If there is no NBI, the second half of the converted symbol will be the replication of the first half due to the FR property of transmitted preamble. In our system model, this is not the case, since we communicate in narrowband interfering environment. We think a band of subcarriers are affected. The power of NBI can be reduced by selecting the un-interfered band to replace the interfered band. This interference elimination process is adapted to the position of center frequency of

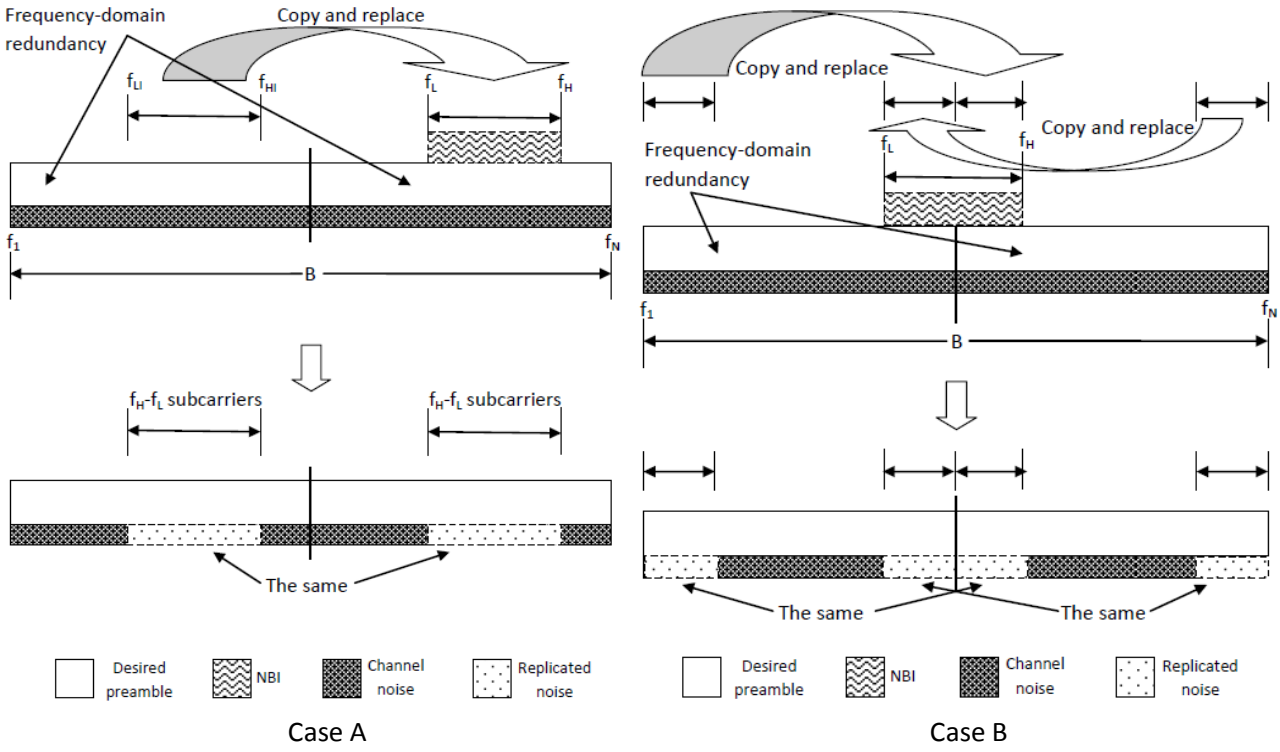

Figure 4. Adaptive band select and replace (ABSR) scheme.

NBI, as shown in Figure 4.

We identify, from ZPS-aided subspace-based NBI detection, the center frequency of NBI. Thus, we recognize the band of NBI-affected subcarriers, assuming a certain percentages of total subcarriers are affected. We consider the case A, where NBI-affected subcarriers are within either the first half or the second half of the preamble symbol. We just copy the corresponding redundant band of subcarriers from the un-interfered half and replace the affected subcarriers. Now, we consider the case B, where where NBI-affected subcarriers are marked out from both halves of the preamble symbol. We can still apply the copy and replace action. We copy the beginning un-interfered part of the first half to replace the beginning interfered part of the second half. Also, we copy the ending un-interfered part of the second half to replace the ending interfered part of the second half. Consequently, we propose adaptive band select and replace (ABSR) algorithm/scheme to eliminate the effect of NBI from preamble symbols. It is apparent that ABSR scheme can eliminate the effect of NBI completely only if the number of NBI-affected subcarriers is less than or equals 50% of total number of subcarriers. Otherwise, ABSR will reduce the effect of NBI partly. In practice, the number of NBI-affected subcarriers is less than or equals 50% of total number of subcarriers.

A side effect is that ABSR causes the replication of part of the channel noise. This will increase the noise power. Conversely, the noise effect will be minimized, since only essential part which is contaminated by the interference is replaced. In this stage, our first task is to find out estimated channels at each subcarrier and then enhancing the estimation accuracy. The block diagram of our proposed approach for NBI-free channel estimation is illustrated in Figure 5. By using least-square (LS) criteria, we have the LS estimation for $\bar{H}$ (Kay, 1993):

$$\hat{\bar{H}}_{LS} = (X^H \times X)^{-1} X^H \bar{Y}, \quad (29)$$

Since X is a diagonal matrix, we have the estimated channel gain of subcarrier k being:

$$\hat{H}_{LS}[k] = \frac{B_k}{X_k}, \quad (30)$$

Where X_k is the transmitted preamble at subcarrier k. Our approach needs a few more steps, which are shown in Figure 6. The LS-estimated channels, using Equation (30), serve the next stage as the preliminary channels. Linear minimum mean squared error (LMMSE) technique minimizes the channel estimation mean square error (MSE) between actual and estimated channel. It has very low MSE, with higher computational complexity, compared with LS estimation. So, we perform low rank LMMSE estimation (Shin et al., 2007) to hold both low MSE, and reduced complexity and this can be expressed as:

$$\hat{\bar{H}}_{trLMMSE} = U \Delta U^H \hat{\bar{H}}_{LS}, \quad (31)$$

Where U and Δ are the unitary and diagonal matrix, respectively. To enhance the estimation further, we apply windowing technique to reduce the spectral leakage. We apply Blackman windowing technique, since our purpose is reducing spectral leakage, but not reserving high resolution. Before windowing, we must perform inverse discrete Fourier transform (IDFT) to get the channel in time

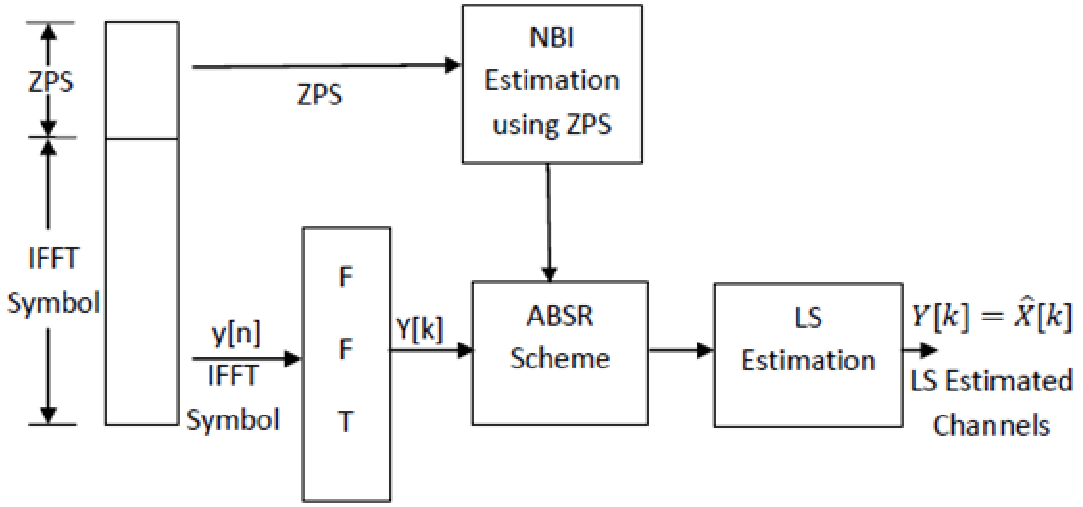

Figure 5. Block diagram of proposed NBI-free channel estimation.

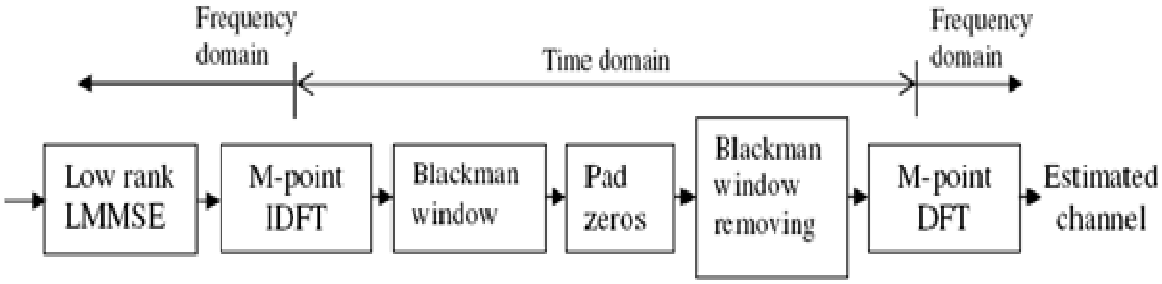

Figure 6. Low rank LMMSE and windowing.

domain and pad zeros, after windowing, and finally remove windowing followed by discrete Fourier transform (DFT). Transforming $\hat{H}_{lrLMMSE}$ into time-domain $h_{lrLMMSE}$ using M-point IDFT, we get:

$$h_{lrLMMSE}(i) = \frac{1}{M}\sum_{k=0}^{M-1} \hat{H}_{lrLMMSE}(k) e^{j2\pi\frac{ki}{M}}, \quad i = 0,1,\ldots,M-1 \tag{32}$$

Blackman window of length M can be expressed as (Blackman et al., 1959):

$$d(i) = 0.42 - 0.5\cos\left(\frac{2\pi i}{M-1}\right) + 0.08\cos\left(\frac{4\pi i}{M-1}\right), \quad i = 0,1,\ldots,M-1 \tag{33}$$

Multiplying Equation (32) by (33), we get the windowed channel as:

$$h_{win}(i) = h_{lrLMMSE}(i).d(i), \quad i = 0,1,\ldots,M-1 \tag{34}$$

Padding N-M zeros, one obtains zero-padded windowed channel as:

$$h_{win-zero}(i) = \begin{cases} h_{win}(i), & 0 \le i \le \frac{M}{2} \\ 0, & else \\ h_{win}(i-N+M), & N-\frac{M}{2} \le N-1 \end{cases} \tag{35}$$

Dividing Equation (35) by (33), one can remove the window. Suppose, this new channel is denoted by $h_{new}(i)$. Applying M-point DFT on $h_{new}(i)$, we obtain the final estimated channels at each subcarrier as:

$$\hat{H}(k) = \sum_{i=0}^{N-1} h_{new}(i) e^{-j2\pi\frac{ki}{N}}, \quad i = 0,1,\ldots,N-1 \tag{36}$$

Now, let us append a description of computational complexity of our proposed method to this section. The number of multiplication is considered as the key source of computational complexity. The conventional LS estimation requires N multiplications, where N is

Table 1. UWB Channel characteristics and corresponding model parameters.

Target channel characteristics and model parameters	CM1 line of sight (LOS): 0 to $4m$	CM2 Non-line of sight (NLOS): 0 to $4m$
Mean excess delay (ns)	5.0	9.94
RMS delay (ns)	5.0	8
Cluster arrival rate ($1/ns$)	0.0233	0.4
Ray arrival rate ($1/ns$)	2.5	0.5
Cluster decay factor	7.1	5.5
Ray decay factor	4.3	6.7
Standard deviation (SD) of cluster lognormal fading term (LNFT) (dB)	3.3941	3.3941
SD of ray LNFT (dB)	3.3941	3.3941
SD of LNFT for total multi-path realization (dB)	3	3

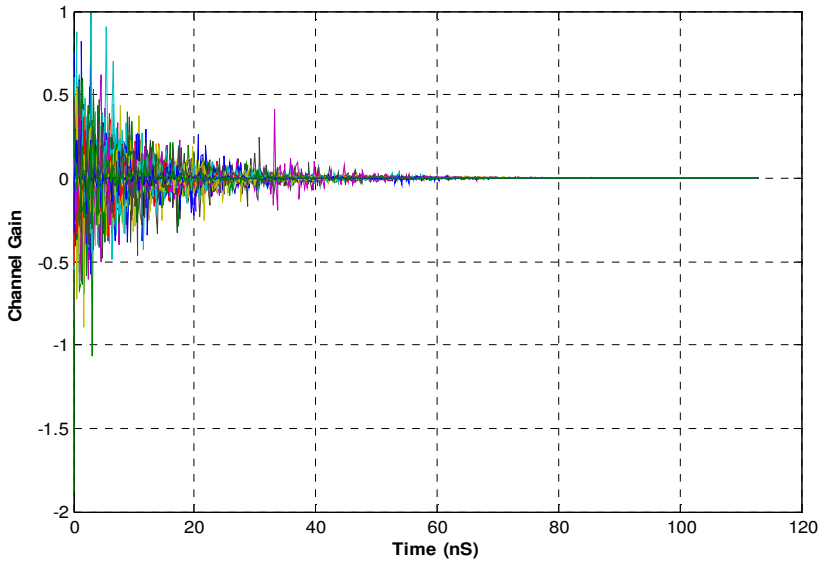

Figure 7. Channel Impulse Response (CIR) realizations for CM1 environment.

the FFT size. Note that the computational complexity of LMMSE is $N^3 + 2 \times N^2$ (Louis, 1991), which is much higher. In case of low rank LMMSE, complexity increase with the optimal rank size p but not with the FFT size. In addition to the complexity of low rank LMMSE, other sources of complexity of our method include IDFT and FFT operations during zero padding through transfer-domain processing. However, it is evident that although the computational complexity of our proposed technique is slightly higher than that of LS approach, this is still considerably less than that of LMMSE approach.

SIMULATION AND RESULTS

Simulation scenario

The criteria of performance assessment is based on the normalized mean square error (NMSE) of channel gain estimation, defined as $\sum_{k=0}^{N-1} |H[k] - \hat{H}[k]|^2 / \sum_{k=0}^{N-1} |H[k]|^2$. The target UWB channel models are CM1 and CM2. Parameters associated with these models are listed in Table 1. Figures 7 and 8 present CIR realization and channel energy characteristic of CM1 model. These characteristics of CM2 Model are represented in Figures 9 and 10. We quantize time in the continuous-time model's (time, value) pairs and hence discrete time model is realized, since the output of the model is a continue time arrival and amplitude value. Frequency hopped (FH) point to point communication is simulated using three frequency bands, where the first symbol is transmitted on a centre frequency of 3432 MHz, the second symbol is transmitted on a centre frequency of

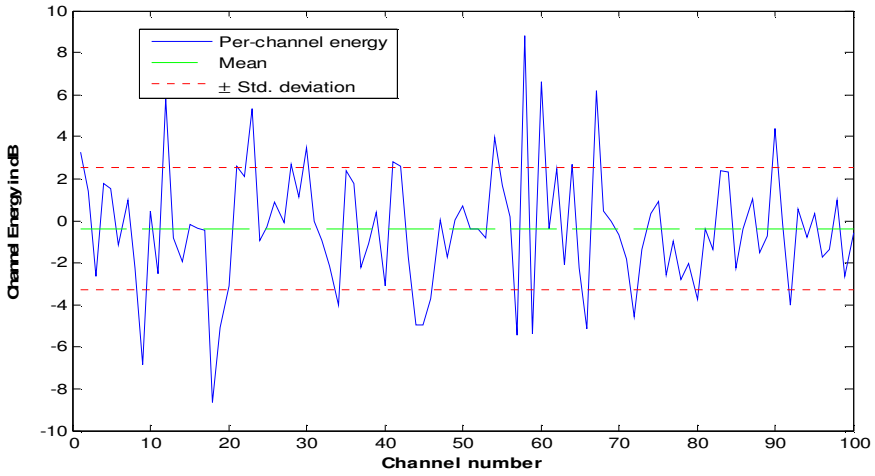

Figure 8. Channel Energy of different channels for CM1 environment.

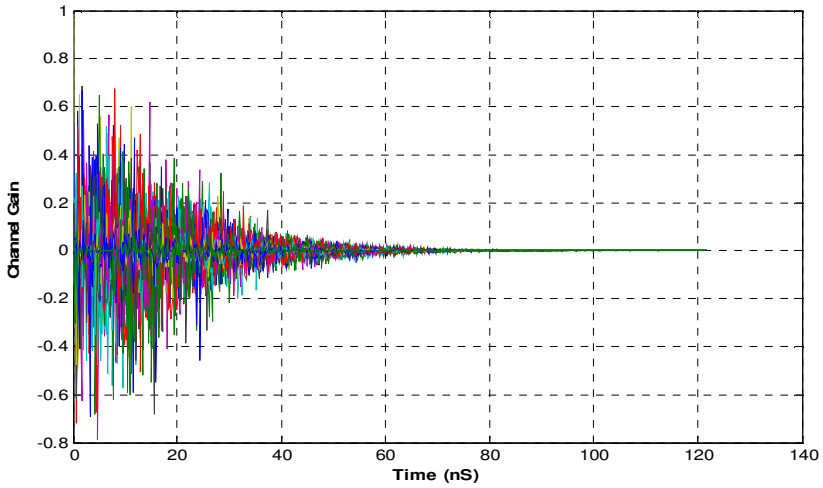

Figure 9. Channel impulse response (CIR) realizations for CM2 environment.

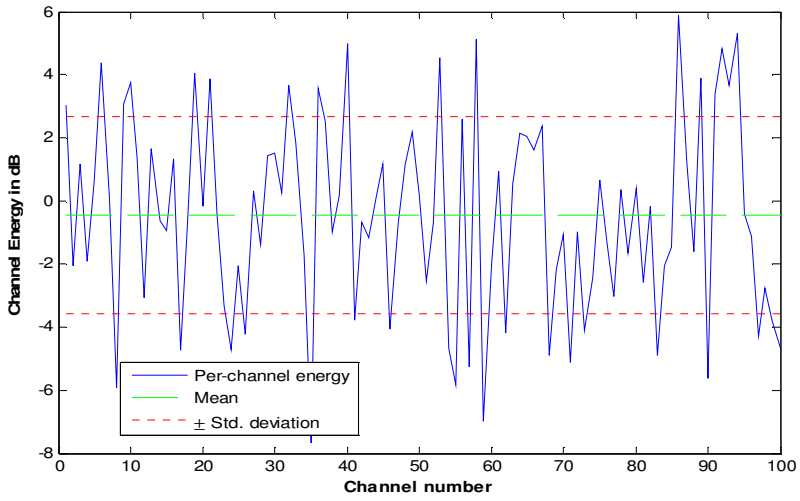

Figure 10. Channel Energy of different channels for CM2 environment.

Table 2. Channel estimation preamble related simulation parameters.

Parameters	Specifications
Frequency bands	Group 1 (band #1-3)
Sampling frequency	528 MHz
FFT size	128
IFFT and FFT period	242.42 (ns)
Number of samples in ZPS	37
ZPS duration in time	70.08 (ns)
Symbol interval	312.5 (ns)
Duration of the channel estimation sequence	$6 \times 312.5\,(ns) = 1.875\,(\mu s)$

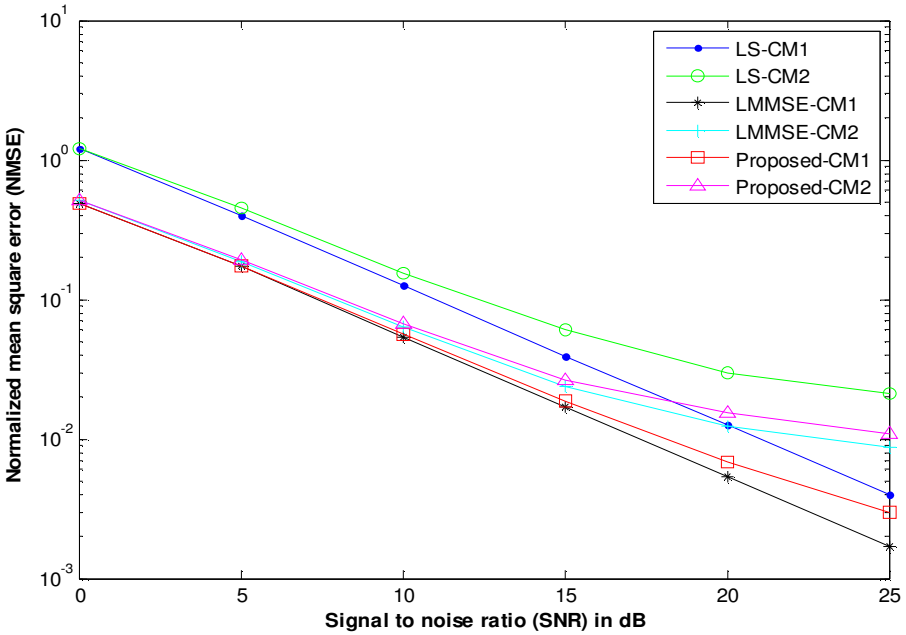

Figure 11. NMSE vs. SNR performance in an NBI-free channel.

3960 MHz, the third symbol is transmitted on a centre frequency of 4488 MHz, the forth symbol is transmitted on a center frequency of 3432 MHz, and so on. All other preamble related parameters, used for channel estimation, are selected according to specifications in (ECMA International, 2008) and are shown in Table 2.

Narrowband interfering environment where more than one interferer could exist is created, considering the frequencies of interferers are positioned in different sub-bands. Thus, existing WiMAX service at 3.5 GHz and WLAN service at 5 GHz are regarded as the interferer to sub-band-1 and sub-band-3, respectively. Also, we assume that severe interfering environment could cause up to 50 percent of total number of subcarriers to become NBI-affected; In fact, this is a case of complete NBI eradication from preambles. Although partial NBI elimination is out of consideration in this article, our technique can effectively be used in such a case also. Simulation results are found from the average of 1000 realizations. Note that we utilize 20-rank LMMSE in our method, since it offers the near-ideal MSE performances in both CM1 and CM2 channel models. MATAB has been utilized as simulation tool throughout our works.

Simulation results

Based on the above simulation scenario, the results we have attained are presented in Figures 11 to 13. In Figure 11, we make available the estimation performances of various methods in terms of mean square error, with an NBI-free channel. Results indicate that our method offers

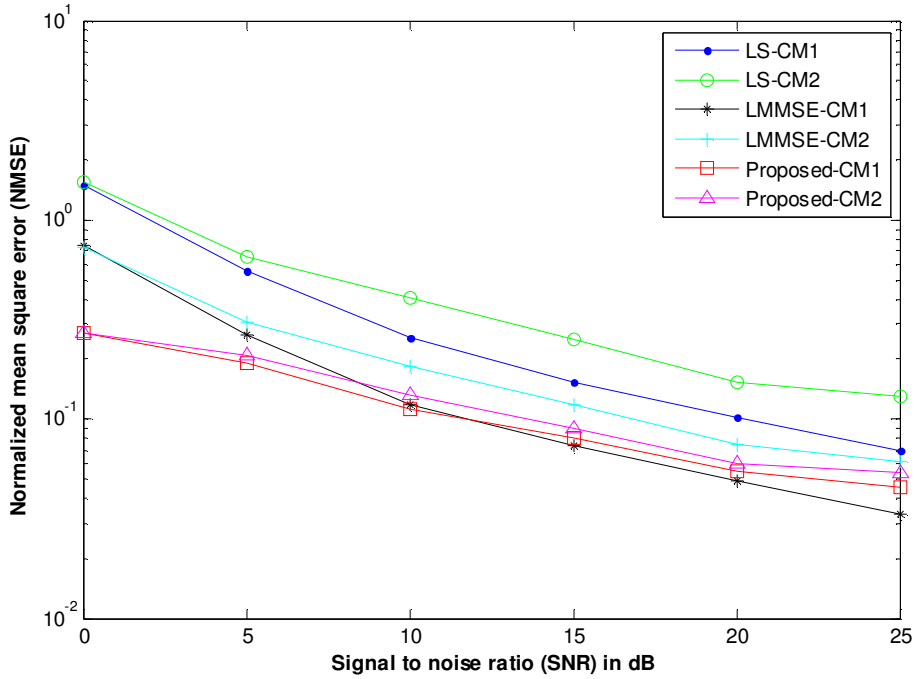

Figure 12. NMSE vs. SNR performance in a channel with moderate NBI.

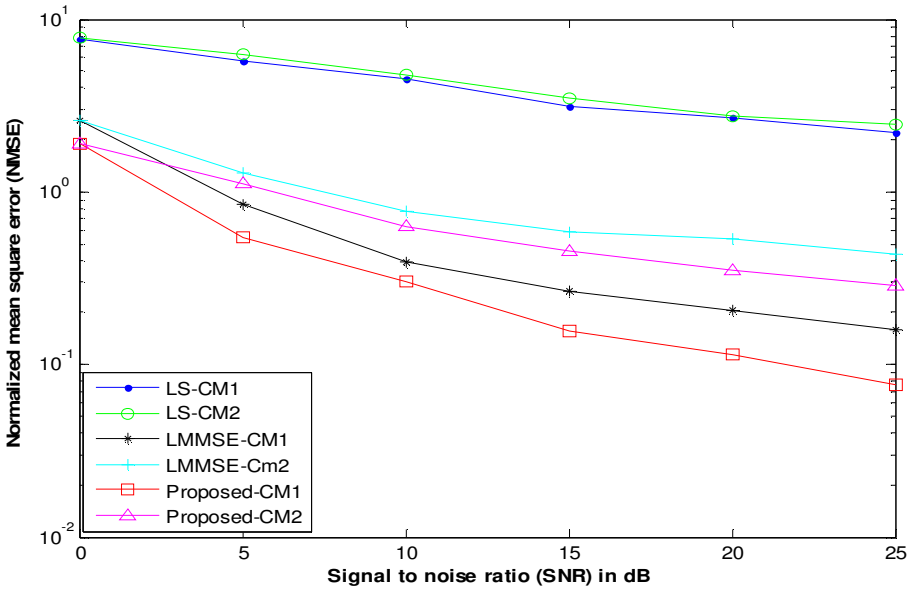

Figure 13. NMSE vs. SNR performance in a channel with sever NBI.

significant performance improvement over LS approach. It also shows that the outcome of proposed method approaches the performance of LMMSE method. In addition to more power at even-numbered preamble samples, post-estimation processing, that is Blackman windowing aid the proposed method to perform better; we made the power, at even-numbered samples of transmitted preamble, double, since odd-numbered samples were decimated. Correlation between neighboring subcarriers in CM1 is differed from that in CM2 and it is because of this that there is a difference between the performance improvement in CM1 and CM2 environments.

Figure 12 shows the NMSE versus SNR performances

of the methods in a moderated interfering channel, that is SIR = 10 dB. In CM1 environment, proposed method outperforms the LMMSE within the range of SNRs up to 11.5 dB. This is because ABSR scheme successfully eliminates NBI from preambles. However, caused by performance saturation of low rank LMMSE, and channel noise enhancement during ABSR scheme, LMMSE starts to exhibit better performance at high SNRs, with the expense of computational complexity. Similar results are found in CM2 environment.

In Figure 13, we compare the performances in a severe interfering environment, that is SIR= -3 μμ. A noticeable performance improvement is occurred, according to this Figure. The LS approach is quite failure to estimate the channel both in CM1 and CM2. We observe that our proposed method reasonably transcends LMMSE approach in terms of NMSE versus SNR performance, since LMMSE suffers from the lack of pre-estimation processing, that is ABSR scheme allowing itself to be dictated by ZPS-aided subspace-based NBI detection.

Conclusion

In this article, we propose a noble channel estimation approach for MB-OFDM UWB system in narrowband interfering environment. This method successfully eliminates the effects of NBI from preambles. The combined action of ABSR scheme and Blackman windowing causes a noticeable performance improvement in a severe interfering environment. Even in an interference-free channel, the proposed method offers significant performance improvement over the LS approach and becomes near-equal to LMMSE approach, since the transmitted power, at even-numbered preamble samples, is allowed to be increased by a factor of 2. Moreover, the use of low rank LMMSE reduces the computational complexity; as a result, this method can become particularly useful in end-user devices. Also, the employ of the parameters, associated with ECMA-368 standard, enables the proposed approach to be successfully used in MB-OFDM UWB system and thus to pioneer UWB-based WPAN.

Coexistence of WLAN or WiMax service and UWB-based WPAN urges an in-depth analysis to evaluate the impacts of a specific service on the performance of channel estimation. In this context, our future work includes the study, analysis and understanding of how a specific existing service affects CFO, which in turn influences the performance of channel estimation.

ACKNOWLEDGEMENTS

This research was supported by the MKE (The Ministry of Knowledge Economy), Korea, under the ITRC (Information Technology Research Centre) support program supervised by the NIPA (National IT Industry Promotion Agency) (NIPA-2010-C1090-1011-0007) and by the National Research Foundation of Korea (NRF) grant funded by Korea government (MEST) (No. No.2010-0018116).

REFERENCES

Blackman RB, Tukey JW (1959). Particular Pairs of Widows: In The measurement of Power Spectra, From the Point of View of Communications Engineering. New York, Dover, pp. 98-99.

ECMA International (2008). Standard ECMA-368: High Rate Ultra Wideband PHY and MAC Standard. ECMA International, 2nd Edition.

Fan X, Leng B, Zhang Z, Bi G (2005). An Improved Channel Estimation Algorithm for OFDM UWB. In Proceedings of IEEE WCNC, New Orleans, LA, USA, pp. 1: 173-176.

Frein CD, Flanagan M, Fagan A (2006). OFDM Narrowband Interference Estimation Using Cyclic Prefix Based Algorithm. 11th International OFDM Workshop, Hamburg, Germany.

Hadaschik N, Zakia I, Ascheid G, Meyr H (2007). Joint Narrowband Interference Detection and Channel Estimation for wideband OFDM. In Proceedings of the European Wireless Conference.

Islam SMR, Kwak KS (2010). A Comprehensive Study of Channel Estimation for WBAN-Based Healthcare Systems: Feasibility of Using Multiband UWB. J. Med. Syst. DOI: 1007/s10916-010-9617-6.

Islam SMR, Kwak KS (2010). Energy-Efficient Channel Estimation for Multiband UWB Systems in presence of Interferences. Int. J. Phys. Sci., 5(15): 2235-2245.

Kay SM (1993). Fundamentals of Statistical Signal Processing: Estimation Theory. Prentice Hall International, Inc., New Jersey, USA, pp. 219-275.

Kelleci B, Fischer TW, Karsllayan AI, Shi K, Serpedin E (2008). Adaptive Narrowband Interference Suppression in Multiband OFDM Receivers. Circuits Syst. Signal Process., 27: 475-489.

Li Y, Minn H, Rajatheva RMAP (2008). Synchronization, Channel Estimation and Equalization in MB-OFDM Systems. IEEE Trans. Wireless Commun., 7(11): 4341-4352.

Li Y, Molisch AF, Zhang J (2006). Practical Approaches to Channel Estimation and Interference Suppression for OFDM-based UWB Communications. IEEE Trans. Wireless Commun., 5(9): 2317-2320.

Louis LS (1991). Statistical Signal Processing: Detection, Estimation and Time Series Analysis. Addison-Wesley Publishing Company.

Molisch A, Foerster J, Pendergrass M (2003). Channel Models for Ultra-wideband Personal Area Networks. IEEE Commun. Mag., 10(6): 14-21.

Nee RV, Prasad R (2000). OFDM for Wireless Multimedia Communications. Artech House, Boston, London.

Png KB, Peng X, Chin F (2008). A Low Complexity Adaptive Channel Estimation Scheme for MB-OFDM System. In Proc. IEEE ICUWB, Germany, 3: 47-50.

Popescu DC, Yaddanapudi P (2007). Narrowband Interference Avoidance in OFDM-Based UWB Communication Systems. IEEE Trans. Commun., 55(9): 1667-1673.

Shi K, Zhou Y, Kelleci B, Fischer TW, Serpedin E, Karsilayan AI (2007). Impacts of Narrowband Interference on OFDM-UWB Receivers: Analysis and Mitigation. IEEE Trans. Signal Process., 55(3): 1118-1128.

Shin S, Yang Q, Kwak KS (2007). Performance Analysis of MB-OFDM System using SVD Aimed LMMSE Channel Estimation. In Proc. IEEE ICUWB, Singapore, pp. 840-844.

Snow C, Lampe L, Schober R (2009). Impacts of WiMAX Interferences on MB-OFDM UWB Systems: Analysis and Mitigation. IEEE Trans. Commun., 57(9): 2818-2827.

Tsai YR, Wang CC, Li XS (2008). Adaptive Channel Estimation for MB-OFDM Systems in Multi-access Interfering Environments. In Proc. IEEE VTC, Singapore, pp. 918-922.

Zhang D, Fan P, Cao Z (2004). Receiver Window Design for Narrowband Interference Suppression in IEEE 802.11a System. IEEE 10th Asia-Pacific Conf. Commun., 2: 839-842.